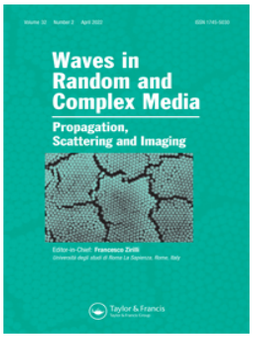

Waves in Random and Complex Media

ISSN: (Print) (Online) Journal homepage: https://www.tandfonline.com/loi/twrm20

Effect of viscous dissipation and thermal radiation on MHD flow and heat transfer for a power-law fluid with variable fluid properties over a permeable stretching sheet

Abeer S. Elfeshawey & Shimaa E. Waheed

To cite this article: Abeer S. Elfeshawey & Shimaa E. Waheed (2022): Effect of viscous dissipation and thermal radiation on MHD flow and heat transfer for a power-law fluid with variable fluid properties over a permeable stretching sheet, Waves in Random and Complex Media, DOI: 10.1080/17455030.2022.2053610

To link to this article: https://doi.org/10.1080/17455030.2022.2053610

Published online: 22 Apr 2022.

WAVES IN RANDOM AND COMPLEX MEDIA
https://doi.org/10.1080/17455030.2022.2053610

Taylor & Francis
Taylor & Francis Group

Effect of viscous dissipation and thermal radiation on MHD flow and heat transfer for a power-law fluid with variable fluid properties over a permeable stretching sheet

Abeer S. Elfeshawey and Shimaa E. Waheed

Department of Mathematics, Faculty of Science, Benha University, Benha, Egypt

ABSTRACT

This manuscript considers the problem of MHD boundary layer flow and heat transfer of power – law fluid with variable fluid properties over a nonlinear stretching sheet in the presence of viscous dissipation and thermal radiation subject to a non-uniform transverse magnetic field and non-uniform heat generation. The governing boundary layer equations are transformed into a system of nonlinear ordinary differential equations using suitable transformation which are solved numerically using fourth order Rung-Kutta integration scheme coupled with the shooting method. The effects of various parameters on the velocity, temperature, local skin-friction and the local Nusselt number are presented and discussed. We found that is as the radiation parameter R increases the temperature of a power-law fluid and the Nusselt number increase, while the viscosity parameter increasing leads to decreasing on the velocity of the fluid and local skin-friction.

ARTICLE HISTORY
Received 3 October 2021
Accepted 10 March 2022

KEYWORDS
Power-law fluid; variable fluid properties; permeable stretching surface; non – uniform heat generation; viscous dissipation

Nomenclature

A,B,c,m,r	constants
A^*, B^*	space and temperature – dependent heat generation /absorption parameter
$B(x)$	magnetic field
B_0	imposed magnetic field(Wbm^{-2})
Cf_x	local skin-friction coefficient
c_p	specific heat at constant pressure$(Jkg^{-1}K^{-1})$
E_c	local Eckert parameter
f	dimensionless stream function
f_w	suction / injection parameter
K	consistency coefficient for power-law fluid (Pas^n)
k^*	mean absorption coefficient
M	magnetic parameter
n	power-law index

CONTACT Abeer S. Elfeshawey abir.mahdy@fsc.bu.edu.eg

Nu_x	local Nusselt number
Pr	generalized Prandtl number
q_r	radiative heat flux
R	radiation parameter
Re_x	local Reynolds number
T	fluid temperature *(K)*
T_{ref}	reference temperature *(K)*
u_w	stretch sheet velocity *(m/s)*
v_w	wall mass transfer velocity*(m/s)*
u, v	velocity component along (x, y) axis *(m/s)*
x, y	Cartesian coordinates *(m)*

Greek symbols

τ_{xy}	shear stress*(Pa)*
κ	thermal conductivity coefficient $(Wm^{-1}K^{-1})$
κ_∞	ambient thermal conductivity $(Wm^{-1}K^{-1})$
μ_∞	ambient dynamic fluid viscosity (Pas^n)
η	similarity variable
ϵ	variable thermal conductivity parameter
α	viscosity parameter
θ	dimensionless temperature
ψ	free stream function(m^2s^{-1})
σ	electric conductivity(Sm^{-1})
σ_1	Stefan–Boltzmann constant
ρ	fluid density(kgm^{-3})

Superscripts

$'$	differentiation with respect to η

Subscripts

w	wall condition
∞	free stream condition

1. Introduction

The study of non – Newtonian fluids has received the attention of many researchers because of its diverse applications, such as food engineering, petroleum production, polymer melt, polymer solutions, etc. In many chemical engineering processes, the most model used in non – Newtonian fluids is the Ostwald-de Wael power law model, where the relationship between the shear stress and the strain rate is

$$\tau_{xy} = K\left|\frac{\partial u}{\partial y}\right|^{n-1}\frac{\partial u}{\partial y}, \tag{1}$$

where τ_{xy} is the shear stress, K is the consistency index and, n is the power-law index. When $(n = 1)$ the fluid is Newtonian, $(n < 1)$ the behavior of the fluid is Pseudo plastic (shear-thinning) and $(n > 1)$ it is the dilutant (shear-thickening) fluid. Several authors investigated the flow and heat transfer of non – Newtonian fluid using Ostwald-de Wael power law model under various conditions [1–19]

In all these above studies, the thermos-physical properties of the ambient fluid are considered to be constant. For lubricating fluids, heat generated by internal friction and the corresponding rise in the temperature affects the physical properties of the fluid, and so the properties of the fluid are no longer assumed to be constant. The increase in temperature leads to boost in the transport phenomena by reducing the physical properties across the thermal boundary layer and the heat transfer at the wall is also affected. Therefore, to predict the flow and heat transfer rates, it is necessary to take into account the variable fluid properties. Many investigators examined the influences of a change in physical properties on flow and heat transfere over several plates [20–24].

The viscosity of a fluid is a measure of its resistance to deformation at a given rate. Viscosity can be conceptualized as quantifying the internal frictional force that arises between adjacent layers of fluid that are in relative motion. It is useful for calculating the force needed to move the fluid which has agreat important in some industries like; petroleum, printing, food and beverages manufactureing. In the area of the flow of an incompressible viscous fluid various aspects of the problem have been investigated [25–32].

The irreversible process by means of which the transformation of kinetic motion of fluid into a thermal energy is defined as viscous dissipation. It has a significant effect on a heat transfer especially for high-velocity flows, highly viscous flows even at moderate velocities, for fluids with a moderate Prandtl number and moderate velocities with small wall-to-fluid temperature difference or with low wall heat fluxes. The effect of viscous dissipation on the hydromagnetic flow and heat transfere for different fluids has been studied by many authors [33–36].

Mahmoud and Megahed [37] examined the effects of viscous dissipation, non-uniform heat generation/absorption on a non-Newtonian power-law fluid flow over a non-linear stretching sheet; They solved the transformed non-linear system of equations using a Shooting method with Runge–Kutta iteration. We will extend the previous study by taking the effects of thermal radiation, variable viscosity and variable thermal conductivity on steady MHD boundary layer flow of an incompressible power-law fluid and heat transfer over a moving nonlinearity stretching sheet in the presence of suction/injection.

2. Mathematical formulation

Consider a steady laminar two-dimensional MHD flow of an incompressible viscous power-law fluid past a non-linearly stretching sheet with variable viscosity and thermal conductivity in the presence of thermal radiation and non-uniform heat generation. Introducing the Cartesian coordinate system, the x-axis extends parallel to the plate, while the y – axis extends upwards, normal to it as shown in Figure 1. A non-uniform magnetic field of strength $B(x) = B_0 x^{\frac{m-1}{2}}$ is applied in the positive y-direction normal to the sheet. It is also assumed that the stretching sheet move with a velocity $u_w(x) = cx^m$.

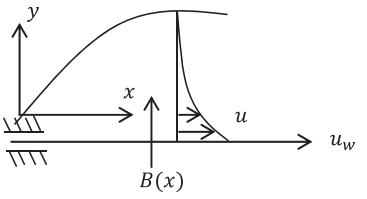

Figure 1. Physical model and coordinate system.

Under the above considerations the steady boundary layer equations governing the flow and heat transfer are:

$$\frac{\partial u}{\partial x}+\frac{\partial v}{\partial y}=0, \tag{2}$$

$$u\frac{\partial u}{\partial x}+v\frac{\partial u}{\partial y}=\frac{1}{\rho}\frac{\partial}{\partial y}\left(K(T)\left|\frac{\partial u}{\partial y}\right|^{n-1}\frac{\partial u}{\partial y}\right)-\frac{\sigma B^2(x)}{\rho}u, \tag{3}$$

$$u\frac{\partial T}{\partial x}+v\frac{\partial T}{\partial y}=\frac{1}{\rho c_p}\frac{\partial}{\partial y}\left(\kappa(T)\frac{\partial T}{\partial y}\right)-\frac{1}{\rho c_p}\frac{\partial q_r}{\partial y}+\frac{\mu}{\rho c_p}\left|\frac{\partial u}{\partial y}\right|^{n+1}+\frac{1}{\rho c_p}q''', \tag{4}$$

subject to boundary conditions

$$y=0: u=u_w(x), v=v_w(x),, T=T_w(x) \tag{5}$$

$$y\to\infty: u\to 0, T\to T_\infty \tag{6}$$

where K and κ are the consistency and the thermal conductivity coefficients respectively and defined as:

$$K=\mu_\infty e^{-\alpha\left(\frac{T-T_\infty}{T_w-T_\infty}\right)}, \tag{7}$$

$$\kappa=\kappa_\infty\left(1+\epsilon\frac{T-T_\infty}{T_w-T_\infty}\right). \tag{8}$$

The non-uniform heat generation (see [38]) is defined as:

$$q'''=\left(\frac{\rho\kappa_\infty u_w}{x\mu_\infty}\right)\left[A(T_w-T_\infty)\frac{u}{u_w}+B(T-T_\infty)\right]. \tag{9}$$

The radiative heat flux q_r is appoint according to the Rosseland approximation [39] so that

$$q_r=-\frac{4\sigma_1}{3k^*}\frac{\partial T^4}{\partial y}, \tag{10}$$

we suppose that the temperature difference within the flow is such that T^4 may be extended in a Taylor's series. Expanding T^4 about T_∞ and drop out the higher orders we get

$$T^4=4T_\infty^3T-3T_\infty^4.$$

The mathematical investigation of the problem is simplified by inserting the following:

$$\eta=\left(\frac{\rho c^{2-n}}{\mu_\infty}\right)^{1/(n+1)}yx^{(m(2-n)-1)/(n+1)},$$

$$\psi = \left(\frac{\mu_\infty c^{2n-1}}{\rho}\right)^{1/(n+1)} x^{(m(2n-1)+1)/(n+1)} f(\eta), \tag{11}$$

$$\theta = \frac{T - T_\infty}{T_w - T_\infty}, T_w = T_\infty - T_{ref}\left(\frac{\rho c^{2-n}}{2\mu_\infty}\right) x^r,$$

where ψ is the stream function that satisfies the continuity Equation (2) defined by

$$u = \frac{\partial \psi}{\partial y},\ v = -\frac{\partial \psi}{\partial x}.$$

and θ is the dimensionless temperature.

Using variables (11) and Equations (7) – (10), the governing Equations (2) – (6) transformed to the following nonlinear ordinary differential equations:

$$ne^{-\alpha\theta}|f''|^{n-1}f''' - \alpha e^{-\alpha\theta}|f''|^n\theta' - mf'^2 + \left(\frac{m(2n-1)+1}{n+1}\right)ff'' - Mf' = 0, \tag{12}$$

$$\frac{1}{Pr}[(1 + R + \epsilon\theta)\theta'' + \epsilon\theta'^2] - r\theta f' + \left(\frac{m(2n-1)+1}{n+1}\right)\theta' f - E_c e^{-\alpha\theta}|f''|^{n+1} + [A^* f' + B^*\theta] = 0, \tag{13}$$

with boundary conditions

$$\eta = 0 : f' = 1,\ f(0) = f_w, \theta(0) = 1, \tag{14}$$

$$\eta \to \infty : f' \to 0, \theta \to 0, \tag{15}$$

where $M = \frac{\sigma B_0^2}{\rho c}$ is the magnetic parameter, $E_c = \frac{\mu_\infty c^n}{\rho c_p T_{ref}} x^{2m-r}$ is the local Eckert parameter, $R = \frac{16\sigma_1 T_\infty^3}{3\kappa^* \kappa_\infty}$ is the radiation parameter, $A^* = \frac{\kappa_\infty}{\rho c_p} A$ and $B^* = \frac{\kappa_\infty}{\rho c_p} B$ are the space and temperature – dependent heat generation/ absorption parameters respectively. It is to be noted that the case $(A^* > 0, B^* > 0)$, corresponds to internal heat generation and that $(A^* < 0, B^* < 0)$, corresponds to internal heat absorption. Also, $Pr = \frac{\rho c_p c}{\kappa_\infty}\left(\frac{\rho c^{2-n}}{\mu_\infty}\right)^{\frac{-2}{n+1}} x^{(1-3m)(1-n)}$ is the generalized Prandtl number, $f_w = -\frac{v_w(x)}{u_w}(Re_x)^{\frac{1}{n+1}}$ is the suction/injection parameter, $Re_x = \frac{\rho x^n (u_w)^{2-n}}{\mu_\infty}$ is the local Reynolds number. It is clear that when $m = \frac{1}{3}$ and $r = \frac{2}{3}$ a similarity solution exist. Therefore the generalized Prandtl number is $Pr = \frac{\rho c_p c}{\kappa_\infty}\left(\frac{\rho c^{2-n}}{\mu_\infty}\right)^{\frac{-2}{n+1}}$ and the Eckert parameter is $E_c = \frac{\mu_\infty c^n}{\rho c_p T_{ref}}$.

The physical quantity of interest in this problem is the local skin friction coefficient C_f and the local Nusselt number Nu_x which can be expressed as

$$\frac{1}{2} C f_x (Re_x)^{\frac{1}{2}} = -e^{-\alpha}|f''(0)|^{n-1} f''(0), \tag{16}$$

$$Nu_x (Re_x)^{-\frac{1}{2}} = -(1 + R + \epsilon)\theta'(0). \tag{17}$$

Table 1. Comparison of the values $-f''(0)$ for various values of n with $m = 1, \alpha = M = f_w = 0$.

	$-f''(0)$	
n	Andersson and Kumaran [40]	Present study
0.5	1.1605	1.0606
0.6	1.0951	1.0950
0.7	1.5450	1.5452
0.8	1.0284	1.0287
0.9	1.0113	1.0111
1	1.0000	1.0000
1.1	0.9924	0.9922
1.2	0.9874	0.9877
1.3	0.9840	0.9839
1.4	0.9819	0.9818
1.5	0.9806	0.9804
1.6	0.9798	0.9798
1.7	0.9795	0.9793
1.9	0.9796	0.9795
2	0.9800	0.9799

Table 2. Comparison of the values $-\theta'(0)$ for various values of B* with $Pr = 10, Ec = 0.1, m = \frac{1}{3}, r = \frac{2}{3}, \alpha = \epsilon = M = f_w = R = A^* = 0$.

	$n = 0.8$		$n = 1.2$	
B*	Mahmoud and Megahed[37]	Present study	Mahmoud and Megahed[27]	Present study
−0.5	3.6846	3.6845	3.6945	3.6946
−0.3	3.3995	3.3994	3.4098	3.4099
−0.1	3.0877	3.0877	3.0986	3.0986
0	2.9192	2.9190	2.9303	2.9303
0.1	2.7401	2.7402	2.7516	2.7517
0.3	2.3403	2.3403	2.3535	2.3533
0.5	1.8544	1.8544	1.8728	1.8728

3. Results and discussion

The system of non-linear ordinary differential Equations (12) and (13) combined with the boundary conditions (14) and (15) were solved numerically using shooting scheme with fourth-order Runge–Kutta iteration. To verify the merit and accuracy of the numerical method, the results of the values of $-f''(0)$ (where $m = 1, \alpha = M = f_w = 0$) for various values of n is compared with those obtained by Andersson and Kumaran [40]. The comparison shows a good agreement with the previous results as seen in Table 1.

Also, another comparison of the values of $-\theta'(0)$ (where $Pr = 10, Ec = 0.1, m = \frac{1}{3}, r = \frac{2}{3}, \alpha = \epsilon = M = f_w = R = A^* = 0$) is carried out with those obtained by Mahmoud and Megahed [37], this comparison confirms that our results have a good agreement with the previous results, see Table 2.

The effects of various parameters on the dimensionless velocity $f'(\eta)$ and the dimensionless temperature $\theta(\eta)$ for both cases of pseudo-plastic fluids ($n = 0.6$) and dilatant fluids ($n = 1.2$) were examined in Figures 2–13, we consider the Prendalt number $Pr = 10$ and $m = \frac{1}{3}, r = \frac{2}{3}$. The variations of $f'(\eta)$ and $\theta(\eta)$ with the generalized power-law viscosity index n is illustrated in Figures 2 and 3 respectively, the dimensionless velocity at the wall

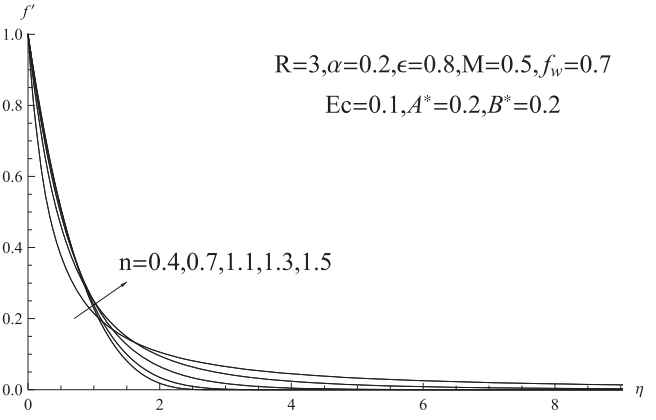

Figure 2. Velocity profiles for various values of *n*.

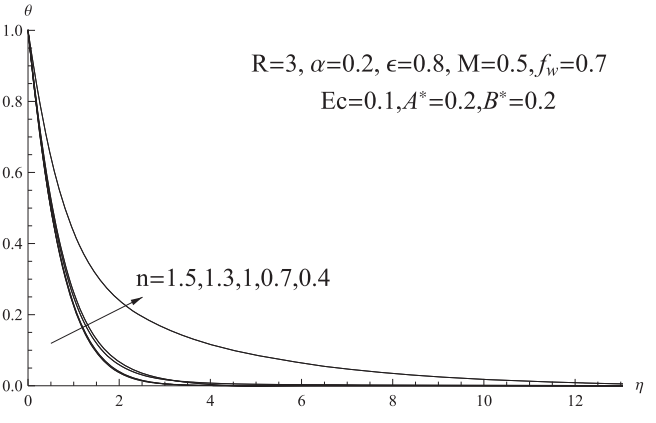

Figure 3. Temperature profiles for various values of *n*.

is increasing with an increase in *n* and the situation is reversed far away from the wall. This because of the fact states that the pseudo-plastic fluids are more amenable to flow than the dilatant fluids. Also, it is seen that the dimensionless temperature decreases as *n* increases.

Figures 4 and 5 represent the dimensionless velocity $f'(\eta)$ and the dimensionless temperature $\theta(\eta)$ for various values of the magnetic parameter *M*, it was observed that the velocity decreases due to the increase of *M*, but the temperature increases due to the increase of *M*. Application of the magnetic field normal to the flow direction gives rise to a resistive drag-like force acting in a direction opposite to that of the flow. This has a tendency to reduce the fluid velocity and increases its temperature.

Figures 6 and 7 illustrate the effects of suction parameter ($f_w > 0$) and injection parameter ($f_w < 0$) on the dimensionless velocity $f'(\eta)$ and dimensionless temperature $\theta(\eta)$, the effect of suction is to decrease the velocity whereas the effect of injection is to increase it. The physical explanation for such a behavior is that suction stabilizes the boundary layer growth, while injection increases the velocity in the boundary layer region, indicating that

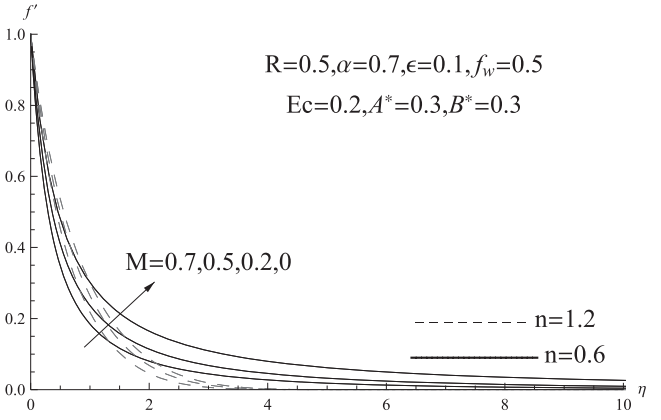

Figure 4. Velocity profiles for various values of *M*.

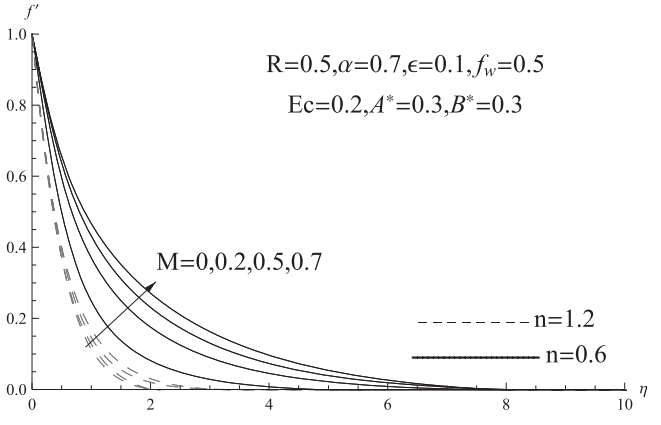

Figure 5. Temperature profiles for various values of M.

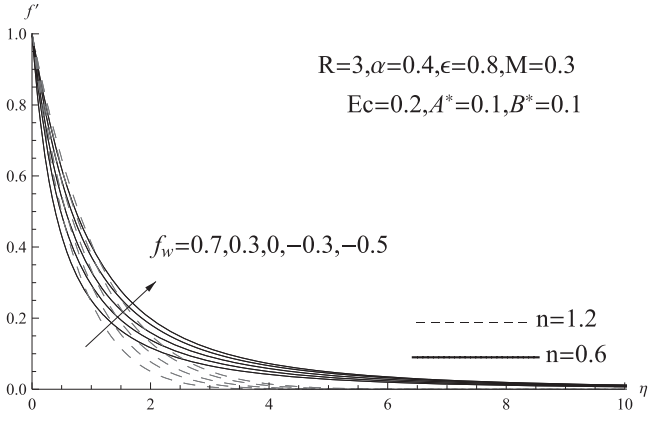

Figure 6. Velocity profiles for various values of f_w.

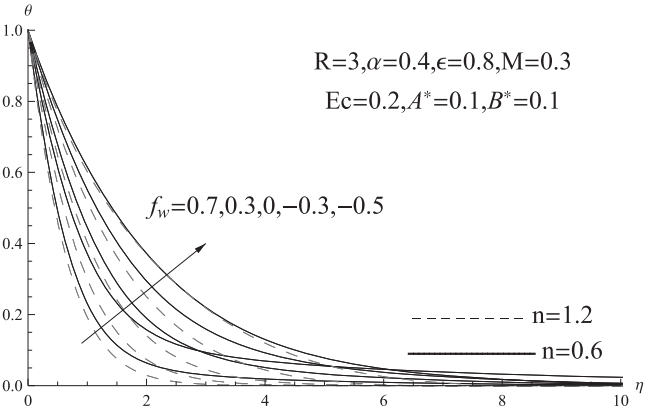

Figure 7. Temperature profiles for various values of f_w.

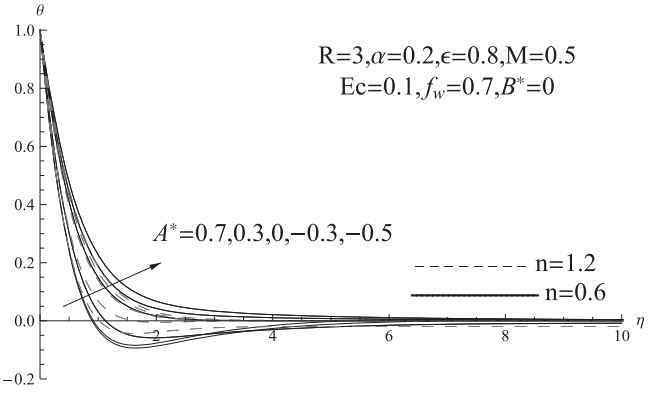

Figure 8. Temperature profiles for various values of A^*.

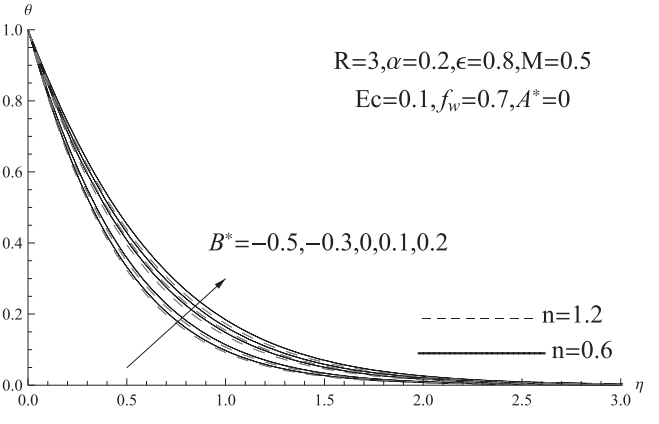

Figure 9. Temperature profiles for various values of B^*.

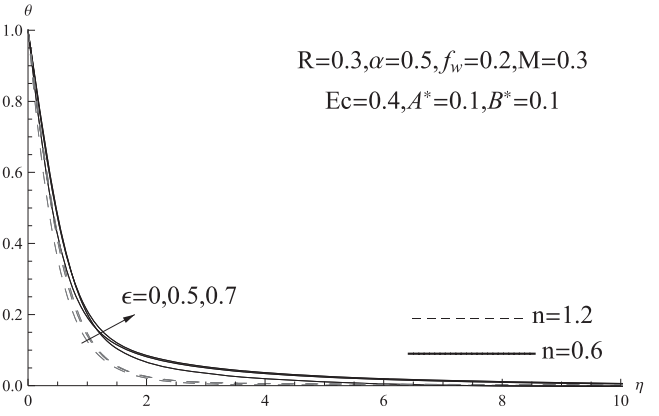

Figure 10. Temperature profiles for various values of ϵ.

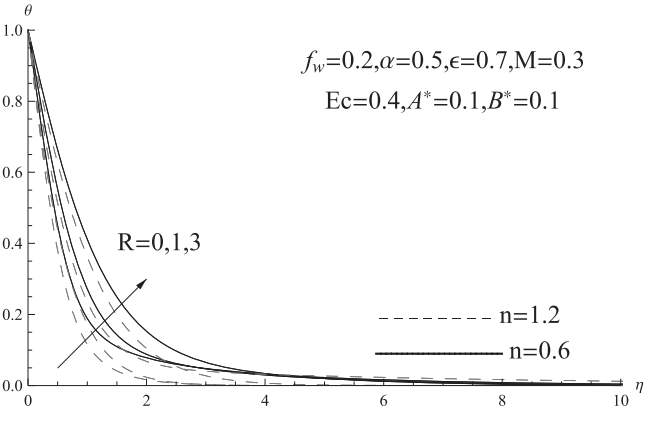

Figure 11. Temperature profiles for various values of *R*.

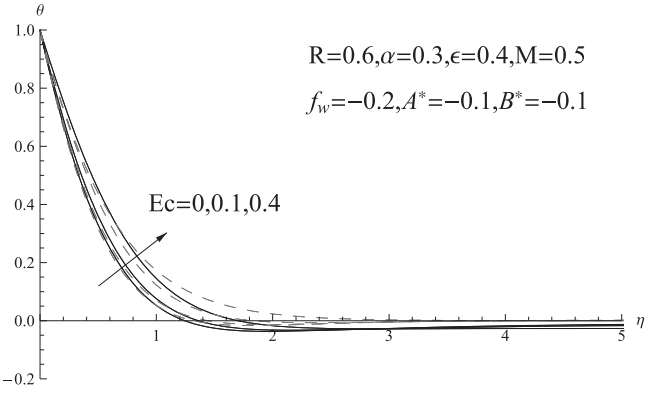

Figure 12. Temperature profiles for various values of *Ec*.

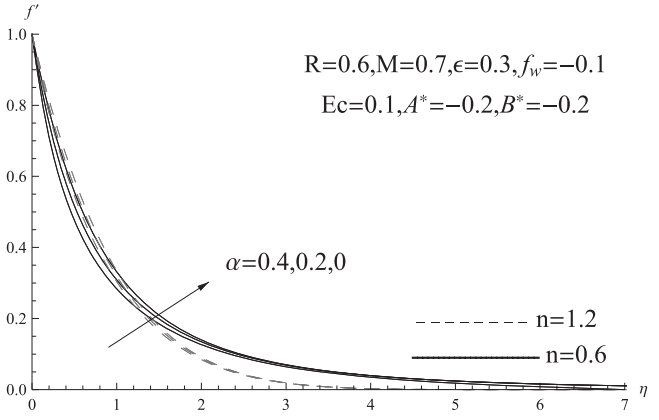

Figure 13. Velocity profiles for various values of α.

injection helps the flow penetrate more into the fluid. This effect is identical to influence on dimensionless temperature $\theta(\eta)$.

Figures 8–12 represent the effects of velocity-dependant heat generation/absorption parameter A^*, temperature-dependent heat generation/ absorption parameter B^*, radiation parameter R, thermal conductivity parameter ϵ and Eckert number Ec on the dimensionless temperature for $(n = 0.6)$ and $(n = 1.2)$. We found that the dimensionless temperature increases with increasing heat generation parameters $(A^* > 0, B^* > 0)$, radiation parameter R, thermal conductivity parameter ϵ and Eckert number Ec. However, increasing heat absorption parameters $(A^* < 0, B^* < 0)$leads to decreasing the dimensionless temperature. But, it is noted that the direction of heat transfer is reversed for negative values of the velocity-dependent heat absorption parameter $(A^* < 0)$.

Finally, the effect of viscosity parameter on the dimensionless velocity is obvious in Figure 13. It is clear that the viscosity parameter has an effect of decreasing the velocity of the fluid. This corresponds to the fact, which states that increasing the viscosity decreases the velocity, which leads to decreasing in the local skin-friction.

To complete our study, we study the effects of the various parameters on the local skin-friction and the local Nusselt number. Table 3 displays this results by assigning numerical values to the magnetic parameter M, suction $(f_w > 0)$ or injection $(f_w < 0)$ parameter, viscosity parameter α, thermal conductivity parameter ϵ, heat generation parameter $(A^*, B^* > 0)$ or heat absorption parameter $(A^*, B^* < 0)$, radiation parameter R and the Eckert number Ec. We noticed that local skin-friction $-Cf_x\sqrt{Re_x}/2$ and Nusselt number $-\mathrm{Nu_x}/\sqrt{\mathrm{Re_x}}$ have the same behaviour for both cases of pseudo-plastic fluids $(n = 0.6)$ and dilatant fluids $(n = 1.2)$. Except the ifluence of the magnetic parameter M on the Nusselt number, we note that is with the magnetic number increasing the Nusselt number increase in pseudo-plastic fluids $(n = 0.6)$ and decrease in dilatant fluids $(n = 1.2)$.

Table 3 shows that, the local skin-friction coefficient increases by increasing the magnetic parameter M, suction parameter $(f_w > 0)$, velocity and temperature-dependent heat absorption parameters $(A^* < 0, B^* < 0)$, while it decreases by increasing the injection parameter $(f_w < 0)$, viscosity parameter α, Eckert number Ec, radiation parameter R,

Table 3. The values of $-\frac{Cf_x\sqrt{Re_x}}{2}$ and $\frac{-Nu_x}{\sqrt{Re_x}}$ with $Pr = 10, m = \frac{1}{3}$ and $r = \frac{2}{3}$ for $n = 0.6$ and $n = 1.2$.

								$-Cf_x\sqrt{Re_x}/2$		$-Nu_x/\sqrt{Re_x}$	
M	f_w	α	R	E_c	ϵ	A^*	B^*	$n = 0.6$	$n = 1.2$	$n = 0.6$	$n = 1.2$
0	0.5	0.7	0.5	0.2	0.1	0.3	0.3	0.7437	0.7348	1.3762	2.8657
0.5								0.9378	0.9666	1.3773	2.6994
1								1.0753	1.1509	1.6743	2.6333
0.3	−0.7	0.4	3	0.2	0.8	0.1	0.1	0.6671	0.5452	2.3948	2.5831
	−0.3							0.7217	0.6115	2.7865	3.0913
	0							0.8143	0.7219	3.5786	3.9893
	0.3							0.9166	0.8450	4.4319	5.0847
	0.7							1.0754	1.0264	6.2020	6.7842
0.7	−0.1	0	0.6	0.1	0.3	−0.2	−0.2	1.1333	0.9997	4.2761	4.4047
		0.2						1.0584	0.9554	4.1798	4.3562
		0.4						0.9803	0.9095	4.0745	4.3051
0.3	0.2	0.5	0	0.4	0.7	0.1	0.1	0.8668	0.7996	2.0397	2.5824
			1					0.8539	0.7865	2.5932	3.1042
			3					0.8389	0.7753	3.3336	3.9807
0.5	−0.2	0.3	0.6	0	0.4	−0.1	−0.1	0.9145	0.8001	3.7370	3.8195
				0.1				0.9111	0.7982	3.4511	3.6094
				0.4				0.9012	0.7928	2.6037	2.9815
0.3	0.2	0.5	0.3	0.4	0	0.1	0.1	0.8720	0.8032	1.9091	2.4357
					0.5			0.8643	0.7973	2.1311	2.6855
					0.7			0.8634	0.7953	2.2500	2.7779
0.5	0.7	0.2	3	0.1	0.8	−0.5	0	1.2503	1.1784	10.7375	10.8792
						−0.3		1.2447	1.1750	9.6610	9.7294
						0		1.2365	1.1710	7.8733	8.1794
						0.1		1.2338	1.1692	7.2769	7.4465
						0.2		1.2313	1.1682	6.6821	7.1409
0.5	0.7	0.2	3	0.1	0.8	0	−0.5	1.2419	1.1746	9.6605	9.9134
							−0.3	1.2400	1.1733	9.0065	9.2769
							0	1.2365	1.1710	7.8733	8.1794
							0.1	1.2350	1.1700	7.4350	7.7568
							0.2	1.2333	1.1688	6.9497	7.2907

thermal conductivity parameter ϵ, velocity and temperature-dependent heat generation parameters ($A^* > 0, B^* > 0$).

Also, from Table 3 we notice that the local Nusselt number increases by increasing suction ($f_w > 0$) parameter, radiation parameter R, thermal conductivity parameter ϵ, temperature and velocity – dependent heat absorption parameters ($B^* < 0, A^* < 0$), this is due to the fact that increasing the heat absorption creates a layer of cold fluid near to the heated surface and therefore the heat transfer rate from the surface increases. Also, it is observed that the local Nusselt number decreases by increasing the injection ($f_w < 0$) parameter, the magnetic parameter M, viscosity parameter α, Eckert number Ec, velocity and temperature-dependent heat generation parameters ($A^* > 0, B^* > 0$), this is because the heat generation mechanism will increase the fluid temperature near the surface and thus temperature gradient at the surface decreases there by decreasing the heat transfer at the plate.

4. Conclusion

There are numerous applications of power-law fluids in various manufacturing industries. Sewage sludge, china clay, oil–water emulsion, cosmetics, paints, synthetic lubricants, biological fluids, jam, jellies, etc.. The present study describes the boundary layer flow and

heat transfer of a non-Newtonian power-law fluid with variable physical properties flow over a stretched sheet under the effects of viscous dissipation, magnetic field, non-uniform heat generation/absorption with a suction/injection. main observations of this study are as follows:

- The behaviour of the velocity, temperature of the fluid, local skin-friction and Nusselt number is similar for both pseudo-plastic fluids and dilatant fluids, except the effect of the magnetic parameter on the Nusselt number, we note that is with the magnetic number increasing the Nusselt number.
- An increase in the values of thermal conductivity parameter leads to an increase in the temperature and the local skin-friction and Nusselt number for Pseudo plastic and dilutant fluids.
- Increasing of the temperature and velocity-dependent heat absorption parameters $(B^* < 0, A^* < 0)$ decrease the dimensionless temperature and increase the local skin-friction and Nusselt number due to createing a layer of cold fluid near to the heated surface which leads to increasing the heat transfer rate from the surface.
- The temperature and velocity-dependent heat generation parameters $(B^* > 0, A^* > 0)$ have the influence of increasing the dimensionless temperature and decreasing the local skin-friction and Nusselt number because the temperature gradient at the surface will increase with increasing the fluid temperature near the surface.

Acknowledgment

This manuscript was produced with the financial support of the Academy of Scientific Research and Technology of Egypt; ScienceUP/GradeUp initiative: Grant Agreement No (6745). Its contents are the sole responsibility of the authors and do not necessarily reflect the views of the Academy of Scientific Research and Technology.

Disclosure statement

No potential conflict of interest was reported by the author(s).

References

[1] Hassanien IA. Flow and heat transfer on a continuous flat surface moving in a parallel free stream of power-law fluid. Appl. Math. Model. 1996;20:779–784.
[2] Howell TG, Jeng DR, De Witt KJ. Momentum and heat transfer on a continuous moving surface in a power law fluid. Inter. J. Heat Mass Trans. 1997;40:1853–1861.
[3] Jadhav B.P. and Wagmode B.B., Approximate solutions of laminar boundary layer flow of power law fluid past a flat plate, J. Ravishanker University, Raipur 1(1988) 185-190.
[4] Tashtoush B, Kodah Z, Al-Ghasem A. On thermal boundary layer of a non-Newtonian fluid on a power-law stretched surface of variable temperature with suction or injection. Heat Mass Trans. 2001;37:459–465.
[5] Aydın O, Kaya A. Laminar boundary layer flow over a horizontal permeable flat plate. Appl. Math. Comput. 2005;161:229–240.
[6] Mahmoud MAA, Mahmoud MAE. Analytical solutions of hydromagnetic boundary layer flow of non-Newtonian power-law fluid past a continuously moving surface. Acta Mech. 2006;181:83–89.
[7] Zheng L, Ting L, Zhang X. Boundary layer flow on a moving surface in otherwise quiescent pseudo-plastic non-Newtonian fluids. Metallurgy. 2008;15:241–244.

[8] Xu H, Liao SJ. Laminar flow and heat transfer in the boundary-layer of non-Newtonian fluids over a stretching flat sheet, compu. Math. Appl. 2009;57:1425–1431.
[9] Cortell R., A note on magneto hydrodynamic flow of a power-law fluid over a stretching sheet, Appl. Math. Comput. 168(2005) 557-566.
[10] Chen CH. Effects of magnetic field and suction/injection on convective heat transfer on non-Newtonian power-law fluids past a power-law stretched sheet with surface heat flux. Int. J. Thermal Sci. 2008;47:954–961.
[11] Ishak A, Bachok N. Steady boundary-layer flow of a non-Newtonian power-law fluid over a flat plate in a moving fluid. Europ. J. Sci. Res. 2009;34:55.
[12] Mahapatra TR, Nandy SK, Gupta AS. Analytical solution of magnetohydrodynamic stagnation-point flow of a power-law fluid towards a stretching surface. Appl. Math. Comput. 2009;215: 1696–1710.
[13] Mahmoud MAA. Slip velocity effect on a non-Newtonian power-law fluid over a moving permeable surface with heat generation. Math. Comput. Model. 2011;54:1228–1237.
[14] Khan WA, Pop I. Flow and heat transfer over a continuously moving flat plate in a porous medium. J Heat Transfer. 2011;133:054501–054501-5.
[15] Postelnicu A, Pop I. Falkner-Skan boundary layer flow of a power-law fluid past a stretching wedge. Appl. Math. Comput. 2011;217:4359–4368.
[16] Mutlag AA, Md J, Ismail AIM, et al. Scaling group transformation under the effect of thermal radiation heat transfer of a non-Newtonian power-law fluid over a vertical stretching sheet with momentum slip boundary condition. Appl. Math. Sci. 2012;6:6035–6052.
[17] Yacob NA, Ishak A. Flow and heat transfer of a power-law fluid over a permeable shrinking sheet. Sains Malaysiana. 2014;43:491–496.
[18] El-Hawary HM, Mahmoud MAA, Abdel-Rahman RG, et al. Group solution for an unsteady non-Newtonian hiemenz flow with variable fluid properties and suction/injection. Chin. Phys. B. 2014;23(9):090203.
[19] Waheed SE, Abu Alnaja KJM. Blowing and suction effects on free convection of a non-Newtonian fluid over a vertical cone embedded in a porous medium in the presence of thermal radiation and non-uniform heat generation/absorption. J. Comput. Theor. Nanosci. 2015;12:1–6.
[20] Seddeek MA, Salama FA. The effects of temperature dependent viscosity and thermal conductivity on unsteady MHD convective heat transfer past a semi-infinite vertical porous moving plate with variable suction, comp. Mater. Sci. 2007;40:186–192.
[21] Mahmoud MAA, Megahed AM. MHD flow and heat transfer in a non-Newtonian liquid film over an unsteady stretching sheet with variable fluid properties. Can. J. Phys. 2009;87:1065–1071.
[22] Patowary G, Sut DK. Study the effect of variable viscosity and thermal conductivity of micropolar fluid in a porous channel. Int. J. Comp. Tech. Appl. 2011;2:1247–1255.
[23] Megahed AM. Variable viscosity and slip velocity effects on the flow and heat transfer of a power-law fluid over a non-linearly stretching surface with heat flux and thermal radiation. Rheol Acta. 2012;51:841–847.
[24] Abdel-Rahman RG, Elfeshawey AS. Thermocapillarity effect on MHD flow for a liquid thin film with variable fluid properties over an unsteady stretching sheet. J. Comput. Theor. Nanosci. 2015;12:4421–4431.
[25] Sreedevi G, Rao RR, Rao DRVP, et al. Combined influence of radiation absorption and Hall current effects on MHD double-diffusive free convective flow past a stretching sheet. Ain Shams Eng. J. 2016;7(1):383–397.
[26] Sreedevi G, Rao DRVP, Makinde OD, et al. Soret and dufour effect on MHD flow with heat and Mass transfer flow past stretching sheet in presence of thermal radiation. IJPAP. 2017;55:551–563.
[27] Sreedevi G. Effects of radiation and chemical reaction on convective nanofluid flow through a Non-linear permeable stretching sheet with partial slip. IJPAP. 2019;57:293–301.
[28] Awan AU, Shah NA, Ahmed N, et al. Analysis of free convection flow of viscous fluid with damped thermal and mass fluxes. Chin J Phys. 2019;60:98–106.
[29] Ali Q, Riaz S, Awan AU. Free convection MHD flow of viscous fluid by means of damped shear and thermal flux in a vertical circular tube. Phys Scr. 2020;95(9):095212.

[30] Ali Q, Riaz S, Awan AU, et al. Thermal investigation for electrified convection flow of Newtonian fluid subjected to damped thermal flux on a permeable medium. Phys Scr. 2020;95(11):115003.
[31] Ali Q, Riaz S, Awan AU, et al. A mathematical model for thermography on viscous fluid based on damped thermal flux. Zeitschrift für Naturforschung A. 2021;76(3):285–294.
[32] Awan AU, Ali Q, Riaz S, et al. A thermal optimization through an innovative mechanism of free convection flow of jeffrey fluid using a non-local kernel. Case Studies in Thermal Engineering. 2021;24:100851.
[33] Cortell R. Suction, viscous dissipation and thermal radiation effects on the flow and heat transfer of a power-law fluid past an infinite porous plate. Chem. Eng. Res. Design. 2011;89:85–93.
[34] Kairi RR, Murthy PVSN, Ng CO. Effect of viscous dissipation on natural convection in a non-darcy porous medium saturated with non-Newtonian fluid of variable viscosity. Open Trans. Ph. J. 2011;3:1–8.
[35] Kishan N, Kavitha P. MHD non-Newtonian power law fluid flow and heat transfer past a non-linear stretching surface with thermal radiation and viscous dissipation. J. Appl. Sci. Eng. 2014;17:267–274.
[36] Chand G, Jat RN. Viscous dissipation and radiation effects on MHD flow and heat transfer over an unsteady stretching surface in a porous medium. Therm. Energy Power Eng. 2014;3:66–272.
[37] Mahmoud MAA, Megahed AM. Non-uniform heat generation effect on heat transfer of a non-Newtonian power-law fluid over a non-linearly stretching sheet. Meccanica. 2012;47:1131–1139.
[38] Dulal P. Combined effects of non-uniform heat source/sink and thermal radiation on heat transfer over an unsteady stretching permeable surface. Cmmun. Nonlinear Sci. Numer.Simulat. 2011;16:1890–1904.
[39] Brewster MQ. Thermal radiative transfer properties. New York: John Wiley &Sons; 1992.
[40] Andersson HI, Kumaran V. On sheet-driven motion of power-law fluids. Int. J. Non-Linear Mech. 2006;41:1228–1234.